

# A Scaling Theory of the Competition between Interdiffusion and Cross-Linking at Polymer Interfaces

A. Aradian\*, E. Raphaël and P.-G. de Gennes  
Physique de la Matière Condensée, C.N.R.S. URA 792,  
Collège de France, 11 place Marcelin Berthelot,  
75231 Paris Cedex 05, France

October 25, 2018

## Abstract

We study theoretically situations where competition arises between an interdiffusion process and a cross-linking chemical reaction at interfaces between pieces of the same polymer material. An example of such a situation is observable in the formation of latex films, where, in the presence of a cross-linking additive, colloidal polymer particles initially in suspension come at contact as the solvent evaporates, and, optimally, coalesce into a continuous coating. We considered the low cross-link density situation in a previous paper (Aradian, A.; Raphaël, E.; de Gennes, P.-G. *Macromolecules* **2000**, *33*, 9444), and presented a simple control parameter that determines the final state of the interface. In the present article, with the help of simple scaling arguments, we extend our description to higher cross-link densities. We provide predictions for the strength of the interface in different favorable and unfavorable regimes, and discuss how it can be optimized.

## 1 Introduction

The purpose of this article is to present a theoretical approach of situations where both interdiffusion and chemical cross-linking occur at the interface between two polymer pieces put in contact at a temperature above their glass transition. Such situations are rather commonplace in polymer processing. More precisely, our main motivation lies in the formation of latex coatings:<sup>1</sup> these contain many such interfaces (of mesoscopic dimensions), and the issue of simultaneous interdiffusion and cross-linking between adjacent polymer particles is crucial for the final properties of the product. As shall be seen, our theoretical description remains rather generic, and should thus, in addition to latex coatings, be of some relevance in other related contexts, like the formation of a (macroscopic) joint between two pieces of rubber.

---

\*Achod.Aradian@college-de-france.fr

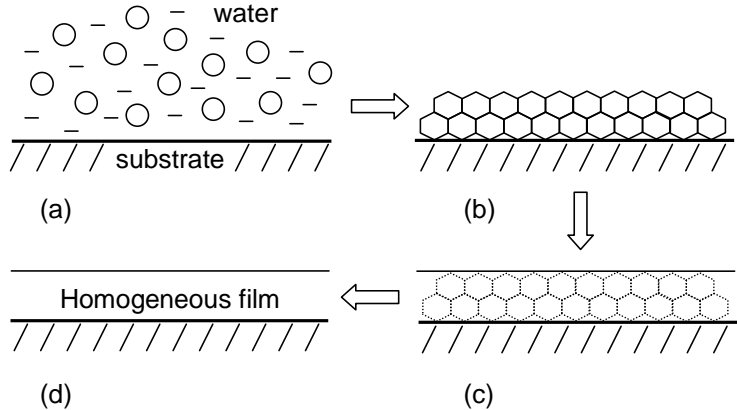


Figure 1: Formation of a latex coating (in the absence of an external cross-linker agent). (a) The initial colloidal dispersion. (b) The particles form a void-free array upon solvent evaporation. (c) Neighbouring particles coalesce, and the initial boundaries faint gradually. (d) Ultimately, the initial granular structure has been lost, and the film is continuous.

The formation steps of latex coatings can be summarized as follows<sup>1</sup> (see Figure 1). A colloidal dispersion of polymer particles in water is applied onto a substrate. As the water evaporates, the particles come into contact, and deform to create a void-free array of polyhedral cells. When good contacts are formed, neighboring particles start to coalesce, i.e. chain interdiffusion takes place at the microscopic scale,<sup>2-7</sup> until, finally, the initial interfaces have “healed” completely. It is also quite usual to add a cross-linker agent into the system (directly in the initial dispersed state),<sup>8,9</sup> with the main goal of improving the bulk properties of the material. However, the introduction of a cross-linker brings along difficulties: at the interfaces between neighboring cells, a competition will arise between the interdiffusion process and the chemical cross-linking reaction, as they will both proceed in parallel. The reason for this fact is simple: since the mobility of polymer chains in the entangled state is drastically reduced by chain branching, the cross-linking slows interdiffusion down. Therefore, the addition of cross-linker into the formulation, by preventing the healing of the interfaces, and even any coalescence at all, may sometimes prove more harmful than beneficial. The central issue in this respect is to control the timing of the chemical reaction.

In a previous paper,<sup>10</sup> we addressed this issue and proposed a control parameter  $\alpha$ , related to the physico-chemical properties of the polymer and the cross-linker. We also discussed two limiting regimes, namely the favorable “slow-reaction” regime and the unfavorable “fast-reaction” regime, and computed the final state of coalescence in the film in each of them. Our study had however a strong limitation: it assumed a very low cross-linker concentration in the system, of the order of *one* cross-linker molecule per chain. Obviously, practical situations are much more

varied — in applications, there is often a much higher cross-link density in the final material. The present article is aimed at extending our description by including this feature. In order to clarify as much as possible the physical content of the theory, we will develop an approach based mainly on scaling arguments.

Our point of view in this article will be that, when a particular application is intended for the material under consideration, one is led to specify requirements on the *bulk* properties of the material. Now, in a quite general fashion, these bulk properties are mainly controlled by the final density of cross-links present in the material. As a consequence, the specifications on the bulk properties impose, in turn, that a given density of cross-links must be incorporated in the material. In what follows, we will thus work with the assumption that the cross-link density has been fixed to a given value beforehand (for “external” reasons) and is a given parameter of the problem. More precisely, we will use the number of monomers between cross-links  $N_c$  (inversely proportional to the density) as a given parameter. We will then provide estimates of the interfacial energy  $G$  under this constraint on  $N_c$ , and see how it can be optimized. In other words, we could say that we try to optimize the interface strength (and all related properties of the material) at given bulk characteristics.

In order to explain this approach of the problem on a more concrete basis, we can invoke again the context of latex coatings. Examples of “bulk related” properties are given by the Young modulus of the coating, the surface hardness, or the extent of swelling in the presence of solvent.<sup>11</sup> Experimentally, these properties are mainly determined by the density of cross-links in the material, and are enhanced as this density increases.<sup>11</sup> For the Young modulus  $E$ , the relation is in fact well-known from the classical theory of rubber elasticity:  $E \sim kT/(N_c a^3)$ , where  $kT$  is the thermal energy,  $a$  the polymer unit (monomer) size and  $N_c$  the number of units between cross-links. On the other hand, there is another set of properties, like the film thickness,<sup>12</sup> the tensile strength,<sup>13</sup> the resistance to scratching and solvent application,<sup>11</sup> or the film homogeneity and aspect, that are rather related to the state of the interfaces. Such “interface related” properties are strongly dependent on the extent of coalescence inside the film, or, equivalently, on the strength of the interfaces (the stronger the interfaces, the better these properties).

We will assume in the rest of this paper that the coalescence and interface strength, which determine the level of the interface properties, are fairly well reflected by the value of the *interfacial adhesion energy*  $G$  between two neighboring particles of the coating. Predictions on this interfacial energy in different regimes constitute the main goal of this work.

The article is organized as follows. In section 2, we derive for a given distance between cross-links  $N_c$ , and with the help of very simple scaling arguments, the control parameter  $\alpha$  that determines the final state of the film. We also compute important quantities like the interpenetration length and the surface density of crossing chains. In section 3, we estimate the interfacial energy  $G$  in different regimes. Finally, in section 4, we discuss our results and present

further perspectives of study.

## 2 A scaling approach to the interdiffusion/cross-linking competition

In this section, we present simple scaling arguments describing the interdiffusion/cross-linking competition at polymer-polymer interfaces. Let us first describe more precisely the physical system under consideration.

### 2.1 Description of the system

In the context of latex coatings, several kind of systems are possible: mixtures of particles of the same or of different polymers (either miscible or immiscible), reaction through functionalized groups on the chains or by addition of a separate cross-linker molecule, etc. As in our previous study, we will here remain with one of the simplest systems of experimental relevance, that is to say, homogeneous particles of the same polymer, and cross-linking by addition of an external chemical reagent. (A brief discussion of other systems is given in section 4.3 of ref. 10.) In the system chosen, all interfaces are identical, and we focus on the evolution of one of them — which amounts to studying the general problem of the competition of interdiffusion and “external” cross-linking at a symmetric polymer/polymer interface.

Let us thus assume that at  $t = 0$ , two pieces of the same polymer material (for instance, two particles from a latex dispersion) are put into contact at a temperature above the glass transition, forming an interface that will be taken to be planar. The polymer pieces are made of a fixed initial network, plus a volume concentration  $\rho_0$  of free chains (which will be able to diffuse across the interface). The free chains are assumed to be linear and monodisperse in the initial state (before the cross-linking reaction starts). In order to remain close to experimental situations, the chains are taken as statistical copolymers of two different units A and  $A^*$ , of which only  $A^*$  may bind with the cross-linker. As a consequence of this chain structure, a quantity that will naturally prove of importance is  $A_0^*$ , the initial volume concentration of  $A^*$ -sites in the system. The total number of units per chain is  $N$ , with  $N$  greater than the entanglement threshold  $N_e \simeq 100$  (entangled state).

The cross-linker agent, X, is bi-functional, and we may split the cross-linking reaction in two stages. The first one is the binding of an X molecule to an  $A^*$ -site borne by a polymer chain  $P_1$ , and can be written as  $P_1A^*+X \rightarrow P_1A^*-X$ . The second step is the effective cross-linking reaction, between a polymer chain  $P_1$  bearing an  $A^*X$ -site, and an  $A^*$  on another chain  $P_2$ , i.e.  $P_1A^*-X + A^*P_2 \rightarrow P_1A^*-X-A^*P_2$ . The first step is quite a fast one, as it involves the diffusion of small X molecules. The second step, a reaction between two macromolecules, will on the contrary be the limiting one. Thus, in the following, we will consider the kinetics of the second stage only, and take for granted that at  $t = 0$ , the first step is completed. As explained already,

the number of monomers between cross-links  $N_c$  (reached when the cross-linking reaction is completed) is fixed, and, we naturally suppose  $N_c \leq N$  (all chains are branched and form a network at the end).

Finally, we consider free, unreacted, chains to be mobile, in contrast with chains that have been subject to branching at some time (due to the cross-linking reaction), which are from that time on considered to be *fixed* at the location of occurrence of the reaction. Such a simplification is not unreasonable, since it is known that the reptation motion of a branched object is exponentially slower than that of a linear one.<sup>14</sup>

## 2.2 The control parameter $\alpha$

Following the tracks of our previous work,<sup>10</sup> we here derive a parameter  $\alpha$ , called the control parameter, which characterizes the final state of the interface (once all chains have reacted and are immobilized). The idea is rather straightforward: the important parameter of the problem is given by the comparison of the rate of the interdiffusion with the rate of the cross-linking reaction. Thus, we define  $\alpha$  as the ratio between the typical interdiffusion time  $T_{\text{diff}}$  and the typical reaction time  $T_{\text{reac}}$ , that is

$$\alpha = \frac{T_{\text{diff}}}{T_{\text{reac}}} \quad (1)$$

There are obviously two limits: when the reaction is much faster than the interdiffusion (“fast-reaction” regime), the chains are locked in place before any significant coalescence can occur. When the reaction is slow enough (“slow-reaction” regime), the interface heals completely before the reaction freezes the system.

The interdiffusion time  $T_{\text{diff}}$  is the time needed to heal completely the initial interface between the pieces in contact, in the absence of reaction. Such a healing occurs when interfacial chains on either side have traveled a distance comparable to their own size inside the neighboring piece of polymer.<sup>2–7</sup> Referring to the theory of reptation,<sup>17,18</sup> the time needed for a chain to travel over its own size is the so-called reptation time  $T_{\text{rep}} = \tau_0 N^3 / N_e$ , (where  $\tau_0$  is a microscopic time typical of molecular agitation). Thus we deduce that

$$T_{\text{diff}} \simeq T_{\text{rep}} = \tau_0 N^3 / N_e \quad (2)$$

We now need to estimate the typical reaction time  $T_{\text{reac}}$ . Quite intuitively, we define this time as the time required to observe *one reaction per chain* in the system. From a scaling law point of view, after this typical time, every chain in the system has undergone branching at least once and is fixed in position: the final state of the film is reached. To evaluate  $T_{\text{reac}}$ , let us follow one  $A^*X$  group on a given chain, chosen at random, and think in terms of a lattice model. Every  $\tau_0$  time intervals, this  $A^*X$  group jumps onto a new site on the lattice, neighboring the one it occupied during the previous time interval. From this new location, the  $A^*X$  is in position to react with all the  $A^*$  lying within a “capture distance”  $b$ , which are, roughly,  $A_0^* b^3$  in number.

However, only a fraction of these “collisions” inside the capture sphere are efficient in giving a true reaction: this is reflected in the value of  $Q$ , defined as the reactivity of the cross-linker, which gives the probability of effective reaction between two partners per unit time spent in collision (that is, as long as their distance is less than the capture radius). Then, as between two jumps the  $A^*X$  sojourns a time  $\tau_0$  on each location, the actual number of reactions at each location is  $Q\tau_0 A_0^* b^3$  (for one  $A^*X$  group). Remembering that each chain contains a number  $N/N_c$  of  $A^*X$  groups, we deduce that the waiting time  $T_{\text{reac}}$  necessary to reach a number of *one* reaction *per chain* is given by the relation  $(N_c/N)Q\tau_0 A_0^* b^3 (T_{\text{reac}}/\tau_0) = 1$ . From that, we obtain

$$T_{\text{reac}} \simeq \frac{N_c}{N} \frac{1}{Q A_0^* b^3} \quad (3)$$

The preceding expression shows that the chemical reaction is all the faster as the cross-linker is concentrated, the chains are long, the cross-linker is reactive and the concentration in sites capable of binding to the cross-linker is high.

The above estimates of the characteristic times finally yield the expression of the control parameter  $\alpha$ :

$$\alpha = \frac{T_{\text{diff}}}{T_{\text{reac}}} \simeq Q\tau_0 A_0^* b^3 \frac{N^4}{N_e N_c} \quad (4)$$

which will serve as a basis for the rest of the article.

For a given system, the two times  $T_{\text{diff}}$  and  $T_{\text{reac}}$  should normally be experimentally measurable (and thus the numerical value of  $\alpha$  could be known in practice). The diffusion time would be easy to determine, as we know from eq. 2 that  $T_{\text{diff}}$  is close to  $T_{\text{rep}}$ . As for the reaction time  $T_{\text{reac}}$ , the unknown quantities are the microscopic reactivity  $Q$  and the capture radius  $b$ . These can be obtained by monitoring the rate of the cross-linking reaction  $A^*X + A^* \rightarrow A^*XA^*$ , and by extracting out the value of the corresponding reaction constant,  $k$ .<sup>19</sup> One can then make use of the physicochemical relation<sup>20</sup>  $k = Qb^3$  to compute directly the value of  $T_{\text{reac}}$  from eq. 3 (the other quantities appearing in the equation being easily measured by other means).

We also note that this formula for  $\alpha$  is the generalization of the one derived in the low cross-linker limit in ref. 10 (which is retrieved by having  $N_c$  as large as allowed, i.e.  $N_c \simeq N$ ).

### 2.3 Interpenetration length and crossing chains density

In section 3, we will compute interfacial adhesion energies that represent the strength of the interface(s). In the process, as explained there, we will need to know two quantities, which are the interpenetration length (the length over which the two polymer pieces forming the joint have mixed), and the crossing density (the density of chains crossing the interface per unit area), at the end of the interface evolution. We now give a scaling derivation of these quantities.

In a way that is consistent with the previous derivation of the control parameter  $\alpha$ , the scaling argument presented here simplifies the kinetics of the chemical reaction as follows: as long as the time  $t$  is less than the reaction time  $T_{\text{reac}}$ , the reaction does not occur, and all initially

free chains remain free. Then, the reaction occurs precisely at  $t = T_{\text{reac}}$ , and after that time, all chains are fixed, meaning that the final state of the film is reached. (More refined calculations validating this scaling approach can be found in ref. 10).

Let us start with the interpenetration length, which is the average thickness that chains from one side of the interface achieve to invade inside the other side. We know from reptation theory<sup>17,18</sup> that, in the entangled state, each chain undergoes a one-dimensional diffusion inside a contorted "tube" representing the topological constraints imposed by the other chains. Thus, in a time  $t$ , a chain travels a curvilinear distance  $S(t) \sim t^{1/2}$  inside the tube. To this contorted distance corresponds a linear, "as the crow flies", distance  $L(t)$ , which can be shown to be proportional to the square root of  $S(t)$  (because the tube shape is a random walk). With the appropriate physical constants, the interpenetration length  $L(t)$  at time  $t$  can be written<sup>3-7</sup>

$$L(t) \simeq \sqrt{aS(t)} \simeq R_0 (t/T_{\text{rep}})^{1/4} \quad (\alpha \ll 1) \quad (5)$$

where  $a$  is the monomer size,  $R_0$  is the Gaussian size of the chains ( $R_0 = aN^{1/2}$ ), and  $T_{\text{rep}}$  is the reptation time ( $T_{\text{rep}} \simeq T_{\text{diff}}$ , see eq. 2). Thus, when the reaction at  $t = T_{\text{reac}}$  brings an end to diffusion, the final interpenetration length is

$$L_{\text{final}} \simeq R_0 (T_{\text{reac}}/T_{\text{rep}})^{1/4} \simeq \frac{R_0}{\alpha^{1/4}} \quad (\alpha \ll 1) \quad (6)$$

and the corresponding contorted distance, really traveled by the chain units along the tube, is

$$S_{\text{final}} \simeq L_{\text{final}}^2/a \quad (\alpha \ll 1) \quad (7)$$

We keep these equations for further use, and now turn to the computation of the density  $\sigma$  of the chains that have crossed the interface (per unit area of surface). To find themselves beyond the interface at time  $t = T_{\text{reac}}$ , these chains were all necessarily not farther than a distance  $L_{\text{final}}$  from the interface, at  $t = 0$ . Assuming that the initial volume concentration of free chains  $\rho_0$  is uniformly distributed inside the material,<sup>21</sup> we deduce that the surface density of crossing chains is

$$\sigma \simeq \rho_0 L_{\text{final}} \quad (\alpha \ll 1) \quad (8)$$

To conclude this section, we should caution that, as indicated, the previous equations are actually valid (and will be used) only for  $\alpha \ll 1$ , that is in the slow-reaction regime. When  $\alpha \gg 1$ , a saturation occurs (for example, in the crossing density  $\sigma$ ), because the rate to which polymer chains enter the interface becomes equal to the rate to which those already present there leave it.<sup>10</sup> However, we do not need to enter into these details, as it is possible to compute the adhesion energy at  $\alpha \gg 1$  without further knowledge.

### 3 Different regimes for the interfacial adhesion energy

We are now in a position to compute the interfacial adhesion energy, which we consider as a fair indicator of the extent of coalescence and the strength developed at the interface. (We remind

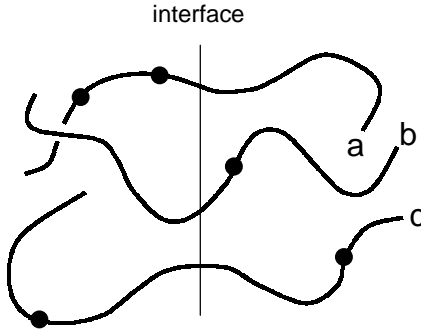


Figure 2: Examples of connector chains. Chains “a” and “b” are tethered only on one side of the interface by chemical bonds (represented by black dots). At the fracture opening, they will be pulled out of the other side. Chain “c” is tethered on both sides, and thus will have to break (scission).

the reader that these quantities are important notably in the context of latex coatings, where they have a strong impact on many properties).

### 3.1 A brief reminder on scission and extraction

The interfacial adhesion energy is the energy one has to provide to open a fracture at the interface between the two polymer pieces at contact (at the end of the interface evolution). Because of visco-elastic dissipation, this energy generally depends on the rate at which the fracture is propagated. We shall here focus on the quasi-static energy  $G$ , i.e. when the rate approaches zero. The energy cost in this limit has two contributions (in elastomers). One is the classical Dupré’s work, valid for all materials (including those made of short molecules), and due to van der Waals interactions. This is a constant offset term that we will henceforth omit. The other contribution is specific to polymers, and comes from the fact that some polymer chains (“connectors”) may cross the interface and extend over both sides, thereby strengthening the joint. This connector contribution itself finds an origin in two distinct processes taking place at the opening of the fracture: chain scission (rupture of chemical bonds) and chain extraction (connectors are dragged out of the surrounding matrix). At zero-detachment rate, whether a given interfacial chain will undergo pull-out or scission depends on whether it is chemically tethered, respectively, on one or both sides of the interface (Figure 2).

Theoretical models are available for both chain scission and extraction. In the case of scission, Lake and Thomas<sup>15</sup> found

$$G_{\text{scission}} \simeq U_0 \tilde{\sigma} \tilde{n} \quad (9)$$

where  $U_0$  is of the order of a typical chemical bond energy (denoted  $U_\chi$ ),  $\tilde{\sigma}$  is the density of

connectors per unit area of interface, and  $\tilde{n}$  is the number of monomers under load along each connector. The physical origin of this expression is that, to rupture a chain between two cross-link points, *each* monomer between these points must be put under load and brought close to the breakage threshold. Hence, to bring a chain to scission, we have to provide an energy  $U_\chi$  to all the  $\tilde{n}$  monomers between the anchorage points. For further use, we note that, in our case, the number of monomers under load is naturally fixed by the separation between cross-links, so that we have  $\tilde{n} \simeq N_c$  (for scission).

We should also immediately point out to avoid later confusion, that the connector density  $\tilde{\sigma}$  is *not* necessarily equal to the crossing density  $\sigma$  given in eq. 8, which concerns polymer chains with  $N$  units: for instance, a chain of  $N$  units that crosses the interface brings (from the adhesion point of view) several connectors made of  $\tilde{n} \simeq N_c$  units. This distinction will be important to obtain a correct estimation of the adhesion energy in some cases.

In the situation of chain extraction, Raphaël and de Gennes<sup>16</sup> found a very similar formula:

$$G_{\text{extraction}} \simeq U_0 \tilde{\sigma} \tilde{n} \quad (10)$$

where  $\tilde{\sigma}$  is the density of connectors to be pulled out,  $\tilde{n}$  the length to be extracted, but this time, the factor  $U_0$  giving the energy scale is a van der Waals bond energy  $U_v$ . Despite the analogy with eq. 9, the physics is quite different: when a chain is extracted, it is exposed to air (interfacial cost) and extended (entropy loss). At room temperature, both contributions to the energy are of the same order:  $U_v$  per monomer.

In mixed situations where during the fracture process, some chains are extracted while others are broken, we will simply assume that the two types of dissipation are additive. However, in such instances, the adhesion energy  $G$  is then often dominated by the chemical part, because  $U_\chi/U_v \simeq 100$ .

### 3.2 Estimation of the interfacial energy $G$

With the above models, we may now estimate the interfacial adhesion energy  $G$  in different regimes. As announced earlier, we will distinguish two regimes depending on the value of the control parameter  $\alpha$ : the slow-reaction regime ( $\alpha \ll 1$ ) and the fast-reaction regime ( $\alpha \gg 1$ ). (It will also appear that the fast-reaction regime is itself divided in two sub-regimes.) We here present calculations, and defer a physical discussion of our findings to the next section.

We start with the slow-reaction regime: the reaction is much slower than the interdiffusion process, which means that the interface has time to heal completely before the chains are stitched. In other words, the interface is allowed to reach the equilibrium state (relative to the interdiffusion process), and, ideally, it is no different from any other plane drawn inside the bulk of the material. Thus, it is natural that the adhesion energy of the interface becomes in this situation equal to the tear energy of the bulk (i.e., the tear energy of a network with a cross-link separation  $N_c$ ). In Figure 3, chain “a” illustrates a typical configuration of interfacial

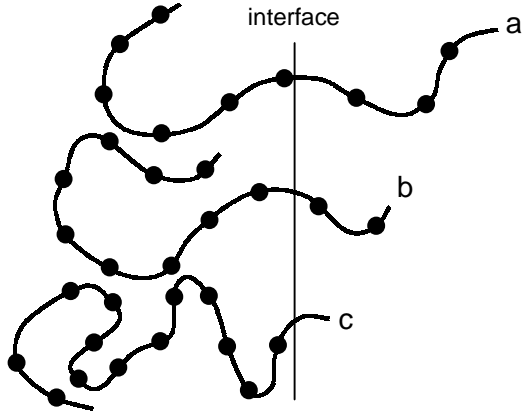


Figure 3: Typical conformations of interfacial chains. Chain “a” is typical of the slow-reaction regime, with arms of comparable size on both sides of the interface. Chain “b” corresponds to the first sub-regime of the fast-reaction regime, with only a small portion of the chain inserted beyond the interface, and will have to rupture at the opening of a fracture. Chain “c” depicts the situation in the second sub-regime, where the inserted portions are even smaller. This chain will rather be extracted from beyond the interface.

chains in this regime. When a fracture is opened, one will have to break (chemically) all these chains that cross the fracture plane, and we can use the Lake and Thomas formula (eq. 9), with a length of the connectors  $\tilde{n} \simeq N_c$ , to estimate the adhesion energy. The chains that cross the interface (and undergo scission) lie inside a Gaussian radius  $a\sqrt{N_c}$  from the fracture, and as the number of chains of length  $N_c$  is  $1/(N_c a^3)$  per unit volume, we deduce that we have  $\tilde{\sigma} \simeq a\sqrt{N_c} \times 1/(N_c a^3) \simeq 1/(\sqrt{N_c} a^2)$  broken connectors per unit area. Thus, the adhesion energy is simply (eq. 9)

$$G \simeq \frac{U_0}{a^2} \sqrt{N_c} \simeq G_{\max} \quad (\alpha < 1, N < N_1) \quad (11)$$

which is the highest possible value in the material (at fixed  $N_c$ ) and is independent of the value of the control parameter  $\alpha$ . We note that eq. 11 refers to values of  $\alpha < 1$ . We may also say that, if all the parameters other than  $N$  are fixed in the expression of  $\alpha$  (eq. 4), this corresponds equivalently to having  $N$  less than a certain threshold  $N_1$  (which we shall compute explicitly later on).

Let us now consider the adhesion energy in the fast-reaction regime: here, the interface has been frozen in an out-of-equilibrium state. In average, chains did not have much time to diffuse across the boundary, and the inserted portions are shorter than in the previous slow-reaction regime (a sketch of a typical chain at the interface in the fast-reaction regime is provided by the chain labeled “b” in Figure 3). Again, there is scission, and the length of the connectors that will be broken at the fracture opening is still  $\tilde{n} \simeq N_c$ . The density of chains crossing the

interface is not at equilibrium, and has the value  $\sigma \simeq \rho_0 L_{\text{final}}$ , as given by eq. 8. However, we should be careful at this point: as announced earlier, this crossing density  $\sigma$  is *not* the density of actual connectors  $\tilde{\sigma}$ . The crossing density  $\sigma$  represents the number of chains of length  $N$  that cross the interface, but, once the cross-links are formed, each of these chains is actually divided into  $N/N_c$  segments of  $N_c$  monomers, and thus gives birth to *several* connectors of length  $N_c$ . To take this fact into account, it can be shown that the crossing density  $\sigma$  must be multiplied by a factor equal to  $L_{\text{final}}/(a\sqrt{N_c})$  to give the actual connector density  $\tilde{\sigma}$  (see the Appendix for a detailed calculation): in computing the adhesion energy, we must thus use  $\tilde{\sigma} \simeq L_{\text{final}}/(a\sqrt{N_c}) \times \sigma \simeq L_{\text{final}}^2 \rho_0/(a\sqrt{N_c})$ . Estimating the initial volume density of free chains roughly as  $\rho_0 \simeq 1/(Na^3)$  (within a numerical prefactor),<sup>22</sup> we find finally

$$G \simeq U_0 N_c \tilde{\sigma} \simeq G_{\text{max}} \frac{1}{\alpha^{1/2}} \quad (1 < \alpha < \alpha_2, N_1 < N < N_2) \quad (12)$$

We see that now the energy displays an inverse dependence in  $\alpha$ , and drops as  $\alpha$  increases.

However, as indicated, the previous equation is valid in a limited range, either in  $\alpha$  ( $\alpha < \alpha_2$ ), or in  $N$  ( $N < N_2$ ) (the critical values  $\alpha_2$  and  $N_2$  will be given shortly). The reason for this is that if the reaction becomes really very fast compared to the interdiffusion (as  $\alpha$  or  $N$  increases), the portions of interfacial chains that are allowed to penetrate into the other side of the interface are extremely short, and become shorter than  $N_c$ . In such conditions, as exemplified by chain “c” in Figure 3, these portions have almost no chance to be cross-linked on both sides of the boundary, and should be rather extracted at the opening of a fracture, implying that we must now consider a sub-regime of the fast-reaction regime where chain extraction predominates inside the adhesion energy (eq. 10). The length  $\tilde{n}$  to be pulled out is of the order of the *curvilinear* length inserted beyond the interface, i.e.  $\tilde{n} \simeq S_{\text{final}}/a \simeq L_{\text{final}}^2/a^2$  (eq. 7). The density of connectors here has no complications: there is only *one* chain end to be extracted per crossing chain, and so each crossing chains makes one connector. (Some chains may have inserted both ends beyond the interface, but this is probably unimportant.) The connector density is thus simply  $\tilde{\sigma} \simeq \rho_0 L_{\text{final}}$  (eq. 8), and altogether, the energy writes, using eq. 10:

$$G \simeq U_0 \frac{L^2}{a^2} \tilde{\sigma} \simeq \frac{U_0}{a^2} N^{1/2} \frac{1}{\alpha^{3/4}} \quad (\alpha > \alpha_2, N > N_2) \quad (13)$$

The inverse dependence of  $G$  in  $\alpha$  in this sub-regime becomes more pronounced.

We now have, with eqs. 11, 12 and 13, a complete estimation of the interfacial adhesion energies in the whole range of the  $\alpha$  parameter. The critical values of  $\alpha$  marking the transitions between the various regimes are:  $\alpha = \alpha_1 = 1$  where we cross-over from the slow- to the fast-reaction regime, and  $\alpha = \alpha_2$  where, inside the fast-reaction regime, we switch from a scission-dominated sub-regime to an extraction-dominated one.

The value of  $\alpha_2$  is easy to determine, since the corresponding transition between sub-regimes is characterized by the fact that the number of monomers inserted beyond the interface by

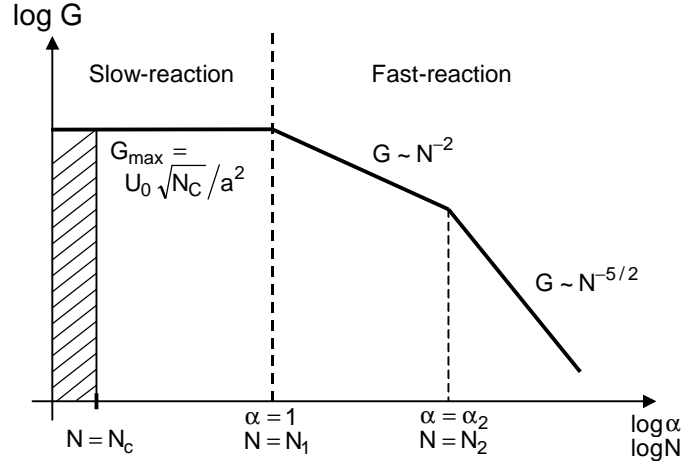


Figure 4: Schematic plot of the adhesion energy  $G$  throughout different regimes (see text), as a function of the control parameter  $\alpha$  or of the chain length  $N$  (in situations where it is the only free parameter). Note that values  $N < N_c$  are not considered as they do not result in the formation of a macroscopic network (gel).

interfacial chains is equal to the number of monomers between cross-links, i.e.  $L_{\text{final}}^2/a^2 = N_c$ . Since  $L_{\text{final}} \simeq R_0/\alpha^{1/4}$  (eq. 6), we deduce that

$$\alpha_2 = \left( \frac{N}{N_c} \right)^2 \quad (14)$$

Alternately, we can also think of these critical  $\alpha$  values as critical values on the chain length  $N$ , if within our given system, the chain length is the only free parameter (all the other parameters entering the expression of  $\alpha$  given in eq. 4 are fixed with known values). The cross-over from slow- to fast-reaction regime sets a first critical length  $N_1$ , which is determined by writing that  $\alpha = 1$  explicitly in terms of all the parameters of the system (eq. 4):

$$N_1 = \left( \frac{N_e N_c}{Q \tau_0 A_0^* b^3} \right)^{1/4} \quad (15)$$

A second critical length, corresponding to  $\alpha = \alpha_2$  and found in the same way, can also be computed:

$$N_2 = \left( \frac{N_e}{Q \tau_0 A_0^* b^3 N_c} \right)^{1/2} \quad (16)$$

A schematic plot of the evolution of the adhesion energy throughout the different regimes is shown in Figure 4 (and will be discussed further in the next section).

## 4 Discussion

### 4.1 Comments on the results of the model

In the previous section, we found several regimes for the final state of the interface: the slow-reaction regime, and the fast-reaction regime (with, for the latter, two sub-regimes). We transit from one regime to another by changing the value of  $\alpha$  in the system, that is to say by changing the respective rates of the interdiffusion and the cross-linking reaction. A special case that may have practical applications is one where all the parameters characterizing the system are fixed, except for the chain length  $N$ . The transitions then occur for two critical values  $N_1$  and  $N_2$ .

The results of the computations of the preceding section can be summarized as follows (see Figure 4). For small  $\alpha$  ( $\alpha < 1$ ) or short chains ( $N < N_1$ ), the interface is granted enough time to reach equilibrium before the reaction occurs. The interfacial strength is in this case maximum, with  $G_{\max} \simeq U_0 \sqrt{N_c}/a^2$ , and is equal to the (ideal) bulk strength. When  $\alpha$  or  $N$  is increased ( $1 < \alpha < \alpha_2$ ,  $N_1 < N < N_2$ ), we enter a regime (fast-reaction regime) where the reaction occurs earlier, and does not allow for full equilibration: the interfacial energy starts decreasing (eq. 12) and displays an inverse dependence on  $\alpha$  and  $N$  of the form  $G \sim \alpha^{-1/2} \sim N^{-2}$ . Finally, if we increase  $\alpha$  or  $N$  further ( $\alpha > \alpha_2$ ,  $N > N_2$ ), the drop in the adhesion becomes even more pronounced (eq. 13):  $G \sim N^{1/2} \alpha^{-3/4} \sim N^{-5/2}$ .

On a practical standpoint, our conclusion is that for an optimized adhesion, i.e., optimized interface-related properties, we need (as expected) to place the system into the slow-reaction regime by a proper choice of the essential parameters involved in  $\alpha$  (or by a proper choice of  $N$  if  $N$  is the only adjustable parameter). If, for some reason, such a proper set of values of the parameters is not accessible experimentally (for example, because the cross-link concentration has been chosen very high, and  $N_c$  is thus very small), we have predictions for the loss in interface energy that should be expected (fast-reaction regime).

At this point, it might be appropriate to give a numerical example. A typical value for the critical chain length  $N_1$  (below which we want to operate) with  $N_e = 100$ ,  $N_c = 500$ ,  $Q\tau_0 = 10^{-9}$ ,  $A_0^* b^3 \simeq A_0^* a^3 = 0.1$  (i.e. one  $A^*$  site every ten polymer units) is found to be (eq. 15):  $N_1 = 4700$  units (a reasonable number). In this case, when  $N < N_1$ , with  $U_0 = 300 \text{ kJ/mol} = 3.1 \text{ eV}$  per monomer and  $a = 5 \text{ \AA}$ , the adhesion energy amounts to  $G_{\max} = 45 \text{ J/m}^2$ .

This value for the adhesion energy is not a very large one, but it must be kept in mind that this is really the lower-bound of observable energies, since it corresponds to a zero-velocity fracture propagation. In practice, much higher values are reached — hopefully, our estimations provide nevertheless useful guidelines toward the most advantageous situations.

### 4.2 The marginal case $N_c \simeq N$

We have worked until now with the assumption that the cross-link density, and, accordingly,  $N_c$ , are determined by the requirements on the bulk properties, and we optimized the interface

strength under this constraint. What happens if the constraint can be relieved, and we are allowed to choose  $N_c$  freely? Suppose that we still want to enhance the interfacial properties: once we have placed ourselves into the slow-reaction regime, with an adhesion energy  $G \simeq U_0\sqrt{N_c}/a^2$ , it is easily seen that  $G$  will increase only if we increase  $N_c$ , i.e. have a looser network with less cross-links. If we really do not care much about the consequences on the bulk strength, we can reduce the cross-link density to the lowest possible value, i.e. two crosslinks per chain ( $N_c = 0.5N$ ): we shall call this limit where  $N \simeq N_c$ , the “marginal case”. (This marginal case was the one we studied in ref. 10.) In the slow-reaction regime, when  $N \simeq N_c$ , the adhesion energy (see eq. 11) becomes  $G \simeq U_0N^{1/2}/a^2$ , and is now an increasing function of the chain length  $N$ . However, if the chain length is increased too much, we fall into the fast-reaction regime again (since  $\alpha$  increases too). There is, however, a minor change as compared to the “usual” fast-reaction regime described in the previous section: the critical chain lengths  $N_1$  and  $N_2$  here collapse one onto the other, so that the first sub-regime (scission) disappears, and we enter directly into the second (extraction-dominated) sub-regime, which can be shown<sup>10</sup> to behave like  $G \sim N^{-7/4}$ .

The whole evolution of  $G$  vs. chain length in this marginal regime is summarized in Figure 5. As can be seen, there is an optimum in the curve at the transition between the slow- and fast-regime. In our approach, this optimum energy is predicted to be the maximum attainable adhesion energy in the system (when all constraints on the bulk properties are released). The optimum chain length  $N_{\text{opt}}$  is found by letting  $\alpha = 1$ ,

$$N_{\text{opt}} \simeq \left( \frac{N_e}{Q\tau_0 A_0^* b^3} \right)^{1/3} \quad (17)$$

and the optimum energy is then simply

$$G_{\text{opt}} \simeq U_0 N_{\text{opt}}^{1/2} / a^2 \quad (18)$$

We should caution, however, that the formulae 17 and 18 are based on extrapolations near  $\alpha = 1$  of the results found at  $\alpha \ll 1$  or  $\alpha \gg 1$ , and should therefore be regarded as tentative.

We may again give a numerical example. For  $N_e = 100$ ,  $Q\tau_0 = 10^{-9}$ , and  $A_0^* b^3 = 0.1$ , we have  $N_{\text{opt}} = 10000$  units. With  $U_0 = 300 \text{ kJ/mol} = 3.1 \text{ eV}$  per monomer and  $a = 5 \text{ \AA}$ , the corresponding energy is  $G_{\text{opt}} = 200 \text{ J/m}^2$ .

We close this section by emphasizing that this “marginal” regime is not very realistic for latex coatings, where a high level of cross-linking is usually desired. But it may be applicable to certain types of low cross-link adhesives.

### 4.3 Concluding remarks and further perspectives

The approach to the competition of interdiffusion and cross-linking at interfaces presented in this article remains clearly very simplified, and we certainly do not hope to provide a fully

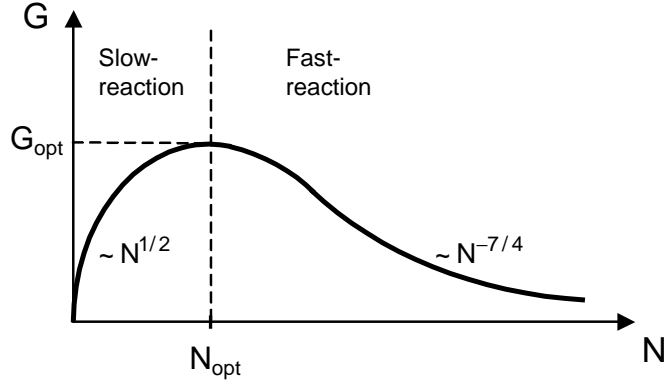


Figure 5: Schematic plot of the adhesion energy  $G$  vs. the chain length  $N$  in the marginal case  $N_c \simeq N$ .

quantitative description of the complexity inherent to real systems. Rather, the goal of this work was to try to extract the essential parameters of such systems, and see how they combine together in governing the dynamics (inside the parameter  $\alpha$ ) or in determining the final state of the interface (inside the adhesion energy  $G$ ).

We should emphasize that the value of the control parameter  $\alpha \simeq Q\tau_0 A_0^* b^3 N^4 / (N_e N_c)$  can in practice be modified by many means: in section 4, we focused on the role of the chain length  $N$ , but this might not be the most relevant procedure from an industrial point of view. One could also change the ratio between “active”  $A^*$ -sites and “passive”  $A$ -sites along polymer chains (thus affecting the concentration  $A_0^*$ ), or change temperature (which would affect both  $Q$  and  $\tau_0$ ). Indeed, in a recent experimental work on latex films,<sup>23</sup> Liu et al. studied (using fluorescence techniques) how the extent of coalescence between neighboring particles varied when the relative rates of interdiffusion and reaction were changed, either by way of temperature, or by adding an acid-catalyst that promoted the cross-linking reaction (i.e., in our language, increased  $Q$ ). It is reasonable to think that this kind of systems would probably provide a direct and powerful approach to test the validity of our model.

To conclude this article, we wish to present now a list of some remaining issues, which, in our view, would have to be understood and included into a comprehensive theory.

To start with, let us recall that we restricted the study to the case of a symmetric interface with two identical polymers facing each other. There are however many other possibilities (we refer the reader to section 4.3 of ref. 10 for the corresponding discussion).

One uncertain point is related to materials with a very high degree of crosslinking, like many industrial latex coatings, where the distance between cross-links becomes significantly smaller than the distance between entanglements ( $N_c \ll N_e$ ): as of now, it is not clear to us whether our approach can be safely extrapolated to such situations, and if not, how it should be amended.

A major issue is also to understand all these situations which have as a common feature to display *inhomogeneities*, as they are in fact ubiquitous in practice. For instance, in latex films, the stability of the initial colloidal dispersion is ensured by coating the individual polymer particles with a layer of a surfactant or a charged polymer. But these surface layers, at the time when the particles come into contact, may significantly affect the interdiffusion dynamics.<sup>24</sup> A closely related difficulty arises when the polymer particles themselves are structured, with a core and a shell that often have very different properties (for example a different  $T_g$ ). Another example where inhomogeneities are crucial is found in the formation of a macroscopic joint between two elastomers: a frequent complication is the formation of an “interphase”, i.e. a region (sometimes fairly broad) around the original interface, where the properties of the material present significant gradients.<sup>25</sup> Quite often, this feature originates in a non-uniform distribution of the cross-linking agent in the initial situation (for example, more abundant at one side of the interface), which then diffuses (with non-uniform concentration) towards the interface. All the interfacial evolution and the final properties become then quite different.

Another unsolved problem arises when the cross-links are not permanent, and have a certain ability to unfasten over long timescales. They may then migrate inside the material and modify the properties of the material in the bulk and at the interfaces.

Chain length polydispersity should also play a role in the competition between interdiffusion and cross-linking. There might be interesting effects, due to the rapid diffusion of smaller chains towards the interface: these might form a “crust” upon cross-linking and considerably modify later diffusion of higher molecular weights fractions.<sup>26</sup> However, at present, we still lack experiments on carefully controlled systems (for example, with bimodal samples containing a mixture of small and long molecules) to draw sound conclusions.

Finally, an interesting line of thought for future work would be to explore analogies (and possible transpositions) of the approach presented here to situations where *phase separation* — rather than coalescence — competes with cross-linking, as in thermoset-thermoplastic blends.<sup>27</sup> These materials are obtained from an initially homogeneous mixture of the thermoplastic polymer with the thermoset precursor. The latter is submitted to a cure, and as the reaction proceeds, the mixture usually destabilizes: a phase separation starts, and enters into competition with the cross-linking reaction, which reduces chain mobility through branching processes. We hope to investigate this aspect in the future.

## Acknowledgements

The authors are indebted to M. Winnik for initiating this work and for many subsequent written and oral exchanges. They would also like to thank C. Creton, L. Lger and M.-F. Vallat for stimulating discussions and comments.

## Appendix. Computation of the connector density $\tilde{\sigma}$

In this appendix, we present an estimation of the density of connectors per unit area of interface  $\tilde{\sigma}$ , which was used to estimate the adhesion energy given in eq. 12 for the fast-reaction regime (more precisely, in the scission-dominated sub-regime delimited by  $1 < \alpha < \alpha_2$ , or, equivalently, by  $N_1 < N < N_2$ ).

In order to make a correct estimation of the connector density, we must consider in some detail the spatial conformation of the chains lying at the interface. Initially (i.e., at  $t = 0$ ), the interfacial chains are contorted because they are not allowed to cross the interface and have to “reflect” on it. Once the contact between neighbouring polymer pieces has been made, they start to relax towards their equilibrium Gaussian conformations (thereby crossing the boundary). However, in the fast-reaction regime under consideration here, these chains have time to relax only partially: only the chain portions that could escape from the initial, “reflected” reptation tube, are finally really able to cross the interface. In average, these relaxed portions have a contour length given by  $S_{\text{final}}$  (eq. 7), and contain a number  $p$  of monomers  $p \simeq S_{\text{final}}/a \simeq L_{\text{final}}^2/a^2$ . Moreover, because of their random shape, each of the relaxed portion crosses the interface *several* times (and not just once as represented, for the sake of pictorial clarity, on Figures 2 and 3). As a consequence, when the reaction occurs and divides all chains into segments of  $N_c$  monomers, a given chain near the interface can, through its relaxed portions, find itself with *several* such segments bridging the interface. In other words, a given chain may contribute, after reaction, to several connectors for the adhesion, and this is why the density  $\sigma$  of chains crossing the interface (eq. 8) differs from the density of connectors  $\tilde{\sigma}$  which is involved in the Lake and Thomas formula for the adhesion energy  $G$  (eq. 9).

We thus have to find out which relation holds between  $\sigma$  and  $\tilde{\sigma}$ , and, for that purpose, the question that must be answered is the following: considering a relaxed chain portion (with  $p \simeq L_{\text{final}}^2/a^2$  monomers) which crosses the interface, how many connectors of  $\tilde{n} \simeq N_c$  monomers does it provide after reaction?

The most convenient method is to divide the polymer chains into “blobs”, which each correspond to a chain segment of  $N_c$  monomers. Such blobs have a (Gaussian) radius  $R_b = aN_c^{1/2}$ . We may now think on the scale of blobs: all relaxed chain portions, with  $p$  monomers, are seen as made with  $p/N_c$  blobs. The idea to find the number of connectors is then simple: we look at the spatial conformation of each chain portion (of blobs), and count how many blobs intersect the interface. Each of these blobs bridges the interface, and, accordingly, must count for one connector. Now, counting the number of such intersections is possible at the scaling law level: it can be shown that if we cut through a random walk of  $q$  links with a virtual plane (passing through the origin of the walk), that plane is intersected an average of  $q^{1/2}$  times. In our case, each relaxed portion of interfacial chain contains  $p/N_c$  blobs, and therefore intersects the interface  $(p/N_c)^{1/2}$  times. Thus, each interfacial chain, through its relaxed portion, provides  $(p/N_c)^{1/2}$  connectors.

The density of *connectors*  $\tilde{\sigma}$  is then simply obtained from the interfacial chain density as  $\tilde{\sigma} = \sigma \times (p/N_c)^{1/2}$ . Substituting with the value  $p \simeq L_{\text{final}}^2/a^2$ , we finally find that the density of connectors  $\tilde{\sigma}$  is given by  $\tilde{\sigma} \simeq \sigma \times L_{\text{final}}/(a\sqrt{N_c})$ , which was precisely the formula used in the main text to establish eq. 12.

## References

- [1] Winnik, M.A. *Curr. Opinion Coll. Interf. Sci.* **1997**, *2*, 192.
- [2] Jones, R.A.L; Richards, R.W. *Polymers at Surfaces and Interfaces*; Cambridge University Press: Cambridge, 1999.
- [3] Wool, R.P. *Polymer Interfaces: Structure and Strength*; Hanser Publications: Cincinnati, 1995.
- [4] de Gennes, P.-G. *C. R. Acad. Sci. Paris, Ser. B* **1980**, *291*, 219.
- [5] de Gennes, P.-G. In *Physics of Polymer Surfaces and Interfaces*; Sanchez, I.C., Fitzpatrick, L.E., Eds.; Butterworth-Heinemann; Manning Publications Co.: London, 1992; p 55.
- [6] Prager, S.; Tirrell, M. *J. Chem. Phys.* **1981**, *75*, 5194.
- [7] Kim, Y.H.; Wool, R.P. *Macromolecules* **1983**, *16*, 1115.
- [8] Bufkin, B.G.; Grawe, J.R. *J. Coatings Technology* **1978**, *50*, No. 641, 41.
- [9] Taylor, J.W.; Winnik, M.A. “Functional Latex and Thermoset Latex Films”. In *Functional Colloids and Fine Particles*; Guyot, A., Ed.; Citus Books: London, 2000.
- [10] Aradian, A.; Raphaël, E.; de Gennes, P.-G. *Macromolecules* **2000**, *33*, 9444.
- [11] Brown, W.T. *J. Coatings Technology* **2000**, *72*, No. 904, 63.
- [12] Zosel, A.; Ley, G. *Macromolecules* **1993**, *26*, 2222.
- [13] Kim, K.D.; Sperling, L.H.; Klein, A.; Hammouda, B. *Macromolecules* **1994**, *27*, 6841.
- [14] de Gennes, P.-G. *J. Phys.* **1975**, *36*, 1199.
- [15] Lake, G.J.; Thomas, A.G. *Proc. R. Soc. London Ser. A* **1967**, *300*, 108.
- [16] Raphaël, E.; de Gennes, P.-G. *J. Phys. Chem.* **1992**, *96*, 4002.
- [17] de Gennes, P.-G. *J. Chem. Phys.* **1971**, *55*, 572.
- [18] Doi, M.; Edwards, S.F. *The Theory of Polymer Dynamics*; Clarendon Press: Oxford, 1986.

- [19] In fact, the most easy way to measure the value of the reaction constant  $k = Qb^3$  would *not* be to monitor the cross-linking reaction  $A^*X + A^* \rightarrow A^*XA^*$  directly in the polymeric system under consideration, but rather in the corresponding *solution of monomers*, i.e. in the solution made of the isolated (not polymerized) A,  $A^*$  and  $A^*X$  molecules.
- [20] (a) O'Shaughnessy, B. In *Theoretical and Mathematical Models in Polymer Research*; Grossberg, A., Ed.; Academic Press: New York, 1998. (b) O'Shaughnessy, B. *Macromolecules*, **1994**, *27*, 3875.
- [21] Assuming a uniform distribution of chain ends in the material amounts to assume that there is no particular attraction or repulsion of chain ends towards the interface in the initial state, which may prove incorrect in certain situations.
- [22] The initial volume density  $\rho_0$  in free chains is reduced when the initial gel fraction in the polymer material is increased. If the initial gel fraction is zero (all the chains are linear and free),  $\rho_0$  becomes maximum:  $\rho_0 \simeq 1/(Na^3)$ . Usually, the gel fraction inside the initial particles is non-zero, but not too high either (a significant amount of free chains must remain to yield good interdiffusion), so that we assume that this diminution of the density of free chains is properly accounted for by placing a purely numerical prefactor in front of that maximum value, without changing the scaling law.
- [23] Liu, R.; Winnik, M.A.; Di Stefano F.; Vanketessan, J. *Macromolecules* **2001**, *34*, 7306.
- [24] Joanicot, M.; Wong, K.; Cabane, B. *Macromolecules* **1996**, *29*, 4976.
- [25] Vallat, M.-F.; Giami, S.; Coupard, A. *Rubber Chem. Technol.* **1999**, *72*, 701. See also references therein.
- [26] Vallat, M.-F. Private communication.
- [27] This possible analogy was brought to the attention of the authors by one of the referees.